

# Adaptive Stress Testing: Finding Failure Events with Reinforcement Learning

**Ritchie Lee**

RITCHIE.LEE@SV.CMU.EDU

**Ole J. Mengshoel**

OLE.MENGSHOEL@SV.CMU.EDU

*Carnegie Mellon University Silicon Valley*

*NASA Ames Research Park, Moffett Field, CA 94035*

**Anshu Saksena**

ANSHU.SAKSENA@JHUAPL.EDU

**Ryan Gardner**

RYAN.GARDNER@JHUAPL.EDU

**Daniel Genin**

DANIEL.GENIN@JHUAPL.EDU

**Joshua Silbermann**

JOSHUA.SILBERMANN@JHUAPL.EDU

*Johns Hopkins University Applied Physics Laboratory*

*11100 Johns Hopkins Rd., Baltimore, MD 20723*

**Michael Owen**

MICHAEL.OWEN@LL.MIT.EDU

*MIT Lincoln Laboratory, 244 Wood St., Lexington, MA 02421*

**Mykel J. Kochenderfer**

MYKEL@STANFORD.EDU

*Stanford University, 496 Lomita Mall, Stanford, CA, 94305*

## Abstract

Finding the most likely path to a set of failure states is important to the analysis of safety-critical systems that operate over a sequence of time steps, such as aircraft collision avoidance systems and autonomous cars. While efficient solutions exist for certain classes of systems, a scalable general solution for stochastic, partially observable, and continuous-valued systems remains challenging. Existing formal and simulation-based methods either cannot scale to large systems or are computationally inefficient. This paper presents adaptive stress testing (AST), a framework for searching a simulator for the most likely path to a failure event. We formulate the problem as a Markov decision process and use reinforcement learning to optimize it. The approach is simulation-based and does not require internal knowledge of the system, making it suitable for black box testing of large systems. We present formulations for both systems where the state is fully observable and partially observable. In the latter case, we present a modified Monte Carlo tree search algorithm, called Monte Carlo tree search for seed-action simulators (MCTS-SA), that only requires access to the pseudorandom number generator of the simulator to overcome partial observability. We also present an extension of the framework, called differential adaptive stress testing (DAST), that can be used to find failures that occur in one system but not in another. This type of differential analysis is useful in applications such as regression testing, where we are concerned with finding areas of relative weakness compared to a baseline. We demonstrate the effectiveness of the approach on an aircraft collision avoidance application, where a prototype aircraft collision avoidance system is stress tested to find the most likely failure scenarios.

## 1. Introduction

Understanding how failures occur is important to the design, evaluation, and certification of safety-critical systems such as aircraft collision avoidance systems (Kochenderfer, Holland, & Chryssanthacopoulos, 2012) and autonomous cars (Bouton, Nakhaei, Fujimura, & Kochenderfer, 2018). The knowledge informs decisions that reduce the probability and impact of failures and prevent loss of

life and property. We consider one of the key problems in failure analysis; we address the problem of finding the most likely sequence of transitions from a start state to a failure state. The problem is challenging in many ways. Many failure events of interest, such as an autonomous car colliding with a pedestrian, cannot be analyzed by considering the system alone. Because failures occur as a result of sequential interactions between the system and its environment, failure analysis must be performed over the combined system. Systems that operate in large, continuous, and stochastic environments thus present modeling and scalability challenges to analysis. The problem is exacerbated because search occurs over a sequence of time steps, which results in an exponential number of possible futures. Exhaustive consideration of all possible paths is generally intractable. In addition to a large search space, failure states can also be extremely rare and hard to reach.

Existing methods can be broadly separated into two categories. Formal verification constructs a mathematical model of the system and rigorously proves or exhaustively checks whether a safety property holds (D’Silva, Kroening, & Weissenbacher, 2008; Kern & Greenstreet, 1999). The properties are expressed using a formal logic, such as linear temporal logic (LTL) (Pnueli, 1977). Probabilistic model checking (PMC) is a formal verification method that verifies properties over stochastic models with discrete state, such as Markov chains and probabilistic timed automata (Katoen, 2016; von Essen & Giannakopoulou, 2016; Gardner, Genin, McDowell, Rouff, Saksena, & Schmidt, 2016). PMC exhaustively evaluates properties over all states and paths subject to probabilistic constraints. Algorithms can prune infeasible paths to reduce the search space (Katoen, 2016). Automated theorem proving (ATP) uses computer algorithms to automatically generate mathematical proofs (Gallier, 2015). Systems and assumptions are modeled in formal logic, and then ATP is applied to prove whether a property holds. If a proof is generated successfully, one can conclude with certainty that the property holds over the entire model. However, if the algorithm fails to generate a proof, then it is uncertain whether the property holds. Hybrid systems theorem proving (HSTP) is a variant of ATP based on differential dynamic logic, which is a real-valued, first-order dynamic logic for hybrid systems (Jeannin, Ghorbal, Kouskoulas, Gardner, Schmidt, Zawadzki, & Platzer, 2015; Kouskoulas, Genin, Schmidt, & Jeannin, 2017). A hybrid system model can capture both continuous and discrete dynamic behavior. The continuous behavior is described by a differential equation and the discrete behavior is described by a state machine or automaton. PMC and HSTP can provide a counterexample when a property does not hold. More importantly, these methods provide completeness guarantees over the entire model, i.e., they can conclude the absence of violations. The major challenge is scalability. Due to their exhaustive nature, they have difficulty scaling to systems with large and complex state spaces. Consequently, applications often make simplifying assumptions, use simplified models, and test subsets of the system (von Essen & Giannakopoulou, 2016; Jeannin et al., 2015).

The second category of methods relies on simulation. These methods rely on the availability of a simulator. Simulation models have very few requirements. They only require the ability to draw samples of the next state. As a result, they can contain large sophisticated models and directly embed software systems. Scenarios can be manually crafted by a domain expert or they can sweep over a low-dimensional parametric model (Chludzinski, 2009). An alternative approach is to run simulations using a stochastic model of the system’s operating environment (Kochenderfer & Chryssanthacopoulos, 2010; Holland, Kochenderfer, & Olson, 2013). Sequences of states are sampled from the simulator and then the sequences are checked for failures. Because sampling is not optimizing for failures, it can take a very large number of simulations to encounter the correct sequence and combination of stochastic values to encounter a failure state. Another problem

is that while this method may find some path to a failure, it does not maximize the probability of the path. Black box optimization algorithms, such as genetic algorithms (GAs), can be applied to direct sampling at a high-level by extracting features from sampled paths and then adjusting testing parameters (Pargas, Harrold, & Peck, 1999; Srivastava & Kim, 2009). Importance sampling and the cross-entropy method have been used to accelerate the discovery of rare events (Kim & Kochenderfer, 2016). However, while these approaches improve upon direct Monte Carlo sampling, they do not leverage the sequential structure of the problem.

This paper presents a method, adaptive stress testing (AST), for accelerating stress testing in simulation. We consider simulators that are Markov processes with discrete time, continuous state, and stochastic transitions. The AST method uses learning to guide sampling of paths so as to optimize finding failure events and maximizing the path probability. It also leverages the sequential structure of the problem for optimization. As a result, it can scale to much larger problems and find failure paths much more efficiently than existing methods. Our AST method formulates the search problem as a sequential decision process and then applies reinforcement learning algorithms to optimize it. We present formulations for both fully observable systems, where the algorithm has full access to the simulator state, and partially observable simulators, where some of the system states are hidden. In the latter case, we present a modified Monte Carlo tree search (MCTS) algorithm, called Monte Carlo tree search for seed-action simulators (MCTS-SA) that only requires access to the pseudorandom number generator of the simulator to overcome partial observability. AST treats the simulator as a black box. As a result, the approach is very general and can be applied to a broad range of systems. We base our algorithm on MCTS because of its ability to scale to large problems and because it can be easily modified to handle non-Markovian systems. Other algorithms can be used as well. For example, deep reinforcement learning has been used for AST to analyze the safety of autonomous cars (Koren, Alsaif, Lee, & Kochenderfer, 2018). Failure scenarios found by AST can then be further analyzed to extract common patterns, e.g., by using an automated categorization algorithm (Lee, Kochenderfer, Mengshoel, & Silbermann, 2018)

In some applications, it may also be very valuable to evaluate failure paths not in absolute terms, but in relation to a baseline system. That is, we are not so interested in cases where both systems fail as cases where the test system fails but the baseline system does not. We call this type of analysis *differential stress testing*. Such situations arise, for example, during regression testing where a new version of a system is compared to a previous one to identify areas of comparative weakness. One way to compare the relative behavior of two systems is to evaluate them against a common set of scenarios. For example, scenarios can be generated by running Monte Carlo simulations using the test system, and then replaying them on the baseline system (Holland et al., 2013). However, this approach suffers from the same inefficiency issues as before. The size and complexity of the state space, the rarity of failures, and the combinatorial explosion of searching over sequences make encountering failure events extremely unlikely. In fact, the issue is even more pronounced in differential stress testing because the failure event needs to occur in the system under test but not the baseline. We present an extension of AST to the differential setting called differential adaptive stress testing (DAST). The approach finds the most likely path to a failure event that occurs in the system under test, but not in the baseline system. DAST follows the same general formulation as AST. However, in the differential setting, we search two simulators in parallel and maximize the difference in the outcomes of the simulators.

We demonstrate the effectiveness of AST and DAST in stress testing the next-generation Airborne Collision Avoidance System (ACAS X) (Kochenderfer et al., 2012). ACAS X is currently

being developed and tested by the Federal Aviation Administration (FAA) to become the next international standard for aircraft collision avoidance. The system will replace the current system, called Traffic Alert and Collision Avoidance System (TCAS), which has performed very well in the past, but is expected to experience operational issues in the next-generation airspace (Kuchar & Drumm, 2007). For example, the number of nuisance alerts is expected to dramatically increase with the rising density of air traffic. As part of the ACAS X team, we obtained various prototypes of ACAS X from the FAA and stress tested them in simulated aircraft encounters to find the most likely scenarios of near mid-air collision (NMAC). Our experiments include single-threat (two-aircraft) encounters, multi-threat (three-aircraft) encounters, and differential stress testing against a TCAS baseline. Our results are reported to the ACAS X development team to inform development and assess risk. In this paper, we highlight the main findings from these reports, along with the novel methods developed.

The remaining sections are organized as follows. Section 2 reviews notation and terminology and background material on sequential decision processes and MCTS. Section 3 presents an overview of the AST framework, followed by formulations of AST for fully observable and partially observable systems. The section also presents the MCTS-SA algorithm for optimizing partially observable systems. Section 4 presents DAST, an extension of AST to differential stress testing. Finally, Section 5 presents our experiments of analyzing near mid-air collisions in an aircraft collision avoidance system.

## 2. Preliminaries

### 2.1 Notation and Terminology

The current state of a simulator  $\mathcal{S}$  is denoted  $s$ , and the next state after a transition is denoted  $s'$ . The action is denoted  $a$ . The *reward*  $r$  is the result of evaluating the reward function on a single transition of the simulator. In cases where the time index is relevant, we use a subscript to indicate the time, e.g., the initial state is  $s_0$ , the state at time  $t$  is  $s_t$ , the action at time  $t$  is  $a_t$ , and the reward at time  $t$  is  $r_t$ . We assume that the simulator is *episodic* in that it terminates in a finite number of steps. The *terminal time*  $t_{end}$  is the first time the simulation enters a terminal state. We assume that terminal states are absorbing so that the simulator remains in the terminal state for all subsequent time steps but does not collect any additional reward. Consequently,  $t \geq t_{end}$  indicates that the simulation has terminated and  $t < t_{end}$  indicates it has not terminated. The simulator terminates either at an event or when a maximum time is reached.

A simulation *path* is a sequence of simulation states from initial to terminal state resulting from a forward simulation. The *total reward*  $R_{total}$  is the sum of the discounted rewards collected over a path, i.e.,  $R_{total} = \sum_{t=0}^{t_{end}} \gamma^t r_t$ . The *event space*  $E$  is the subset of the state space where the event of interest occurs. While this paper focuses on failure events, an event can be arbitrarily defined. We use the notation  $s \in E$  to indicate that an event has occurred. Alternatively, we may use the Boolean variable  $e$  to indicate whether an event has occurred. A *pseudorandom seed*, or just *seed*, is a vector of integers used to initialize a pseudorandom number generator. We assume that all random processes in the simulator are derived from the pseudorandom number generator and seed, so that the result of sampling from these processes is deterministic given the seed.

## 2.2 Sequential Decision Process

A sequential decision process is a mathematical framework for modeling situations where an agent makes a sequence of decisions in an environment to maximize a reward function (Kochenderfer, 2015). If the environment is known and its state is fully observable, then the problem can be formulated as a Markov decision process (MDP). Formally, an MDP is a 5-tuple  $\langle S, A, P, R, \gamma \rangle$ , where  $S$  is a set of states;  $A$  is a set of actions;  $P$  is the transition probability function, where  $P(s' | s, a)$  is the probability of choosing action  $a \in A$  in state  $s \in S$  and transitioning to next state  $s' \in S$ ; and  $R$  is the reward function, where  $R(s, a, s')$  is the reward for taking  $a$  in  $s$  and transitioning to  $s'$ . We define the transition function  $T$  for convenience, where  $T(s, a)$  samples the next state  $s'$  from the distribution  $P(s' | s, a)$ . The parameter  $\gamma \in [0, 1]$  is the discount factor that governs how much to discount the value of future rewards. In an MDP, the agent chooses an action  $a$  at time  $t$  based on observing the current state  $s$ . The system evolves probabilistically to the next state  $s'$  according to the transition function  $T(s, a)$ . The agent then receives reward  $r$  for the transition. The assumption that the transition function depends only on the current state and action is known as the *Markov property*. In cases where the underlying process is Markov, but the agent only observes part of the state, the problem is a partially observable Markov decision process (POMDP) (Kochenderfer, 2015). Instead of choosing  $a$  based on observing  $s$ , the agent chooses  $a$  based on an observation  $o \in O$ , where  $O$  is the set of all possible observations and  $o$  depends on  $s$ . This paper considers models that have a finite number of steps and we set  $\gamma = 1$ .

Reinforcement learning algorithms can be used to optimize sequential decision problems through sampling of the transition function  $T$  (Sutton & Barto, 1998; Wiering & van Otterlo, 2012). The learners adapt sampling during the search, enabling them to efficiently search large and complex state spaces. Value-based reinforcement learning algorithms are a class of learning algorithms that aim to estimate the *state-action value function*  $Q(s, a)$ , which is the expected sum of rewards resulting from choosing action  $a$  in state  $s$  and following an optimal policy  $\pi^*(s)$  thereafter. The *optimal action*  $a^*$  is the action that maximizes the state-action value function at state  $s$ , i.e.,  $a^* = \operatorname{argmax}_a Q(s, a)$ . The *optimal policy*  $\pi^*(s)$  is the function that gives the optimal action  $a^*$  for each state  $s$ . The objective of reinforcement learning algorithm is to find the optimal policy  $\pi^*(s)$ .

## 2.3 Monte Carlo Tree Search

Monte Carlo tree search (MCTS) is a state-of-the-art heuristic search algorithm for optimizing sequential decision processes (Kocsis & Szepesvári, 2006; Browne, Powley, Whitehouse, Lucas, Cowling, Rohlfshagen, Tavener, Perez, Samothrakis, & Colton, 2012). MCTS incrementally builds a search tree using a combination of directed sampling based on estimates of the state-action value function and undirected sampling based on a fixed distribution, called *rollouts*. During the search, sampled paths from the simulator are used to incrementally estimate  $Q(s, a)$  and the optimal policy at nodes in the tree. To account for the uncertainty in the estimates, which may lead to premature convergence, MCTS encourages exploration by adding an exploration term to the state-action value function to encourage choosing paths that have not been explored as often. The exploration term optimally balances the selection of the best action estimated so far with the need for exploration to improve the quality of current value estimates. By doing so, MCTS adaptively focuses the search towards more promising areas of the search space. The effect of the exploration term diminishes as the number of times the state is visited increases.

This paper uses a variant of MCTS called Monte Carlo tree search with double progressive widening (MCTS-DPW), which extends MCTS to large or continuous state and action spaces (Couëtoux, Hooek, Sokolovska, Teytaud, & Bonnard, 2011). When the state and action spaces are large (or infinite), visited states and actions are not revisited sufficiently through sampling alone, which hinders the quality of value estimates. The benefit of MCTS-DPW’s progressive widening is that it forces revisits to existing states and slowly allows new states to be added as the total number of visits increase. Progressive widening stabilizes value estimates and prevents explosion of the branching factor of the tree.

### 3. Adaptive Stress Testing

Adaptive stress testing (AST) aims to find the most likely path from a start state to a failure state in a discrete-time simulator (Lee, Kochenderfer, Mengshoel, Brat, & Owen, 2015). We formulate the search as a sequential decision-making problem and then use reinforcement learning to optimize it. Since one of the main applications of this work is the stress testing of safety-critical systems, we take the view that the simulator can be decomposed internally into the system under test and a stochastic model of its environment. However, this view is not required, and the formulations and algorithms presented in this paper can be applied without modification in either case.

Figure 1 illustrates the general AST framework. A simulator  $S$  models the system under test and the environment. A reinforcement learner interacts with the simulator over multiple time steps to maximize the reward it receives. At each time step, the learner makes an observation, takes an action based on the observation, and receives a reward. The reward function is crafted to both encourage failure events and maximize transition probability. In other words, the overall goal of the reinforcement learner is to search for a sequence of actions that is most *adversarial* to the system under test. The output of the optimization is the most likely sequence of state transitions that results in a failure event.

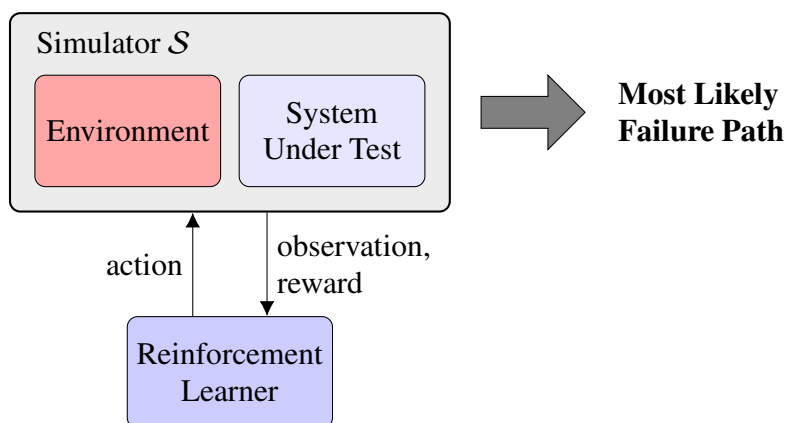


Figure 1: Adaptive stress testing. A reinforcement learner interacts with a simulator and chooses actions to maximize the rewards received. The reward function rewards failure events and state transitions with higher probability.

### 3.1 Full Observability

When the state of the system is fully observable, we can formulate the problem as a Markov decision process (MDP). Figure 2 illustrates the AST framework for the fully observable case. The state  $s$  of the MDP is the state of the simulator, which includes both the state of the environment and the state of the system under test. At each time step, the agent observes the simulator state  $s$  and chooses an action  $a$  based on  $s$ . The system then transitions to the next state and the agent receives a reward. We define the agent’s actions to be the values of the stochastic variables in the simulator. The agent’s action directly sets the values of the stochastic variables and the probability of the assignment, i.e., the probability of the chosen action occurring naturally, is included in the reward function. Our choice of action makes the simulator transition deterministic given the current state and action. We assume a finite horizon problem and set  $\gamma = 1$ .

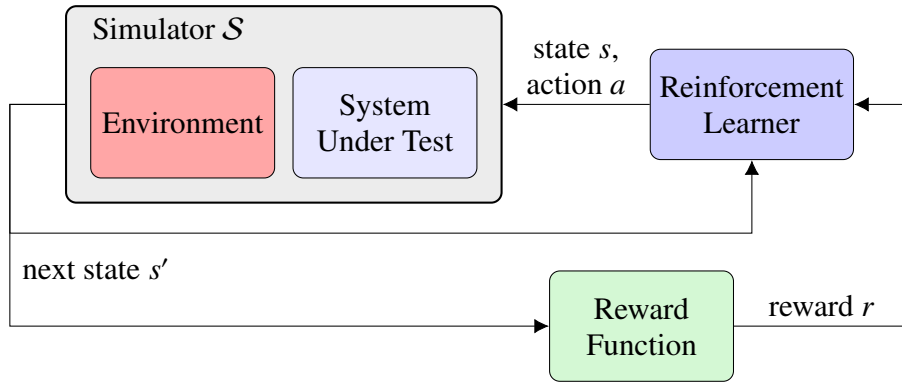


Figure 2: Adaptive stress testing of a fully observable system. The problem is modeled as an MDP where the agent observes the state and chooses an action at each time step. The agent’s action instantiates the stochastic variables in the simulator and the probability of the assignment is included in the reward function. Traditional reinforcement learning algorithms can be applied to solve the MDP.

**Reward Function.** The reward function is designed to find failure events as the primary objective and maximize the path probability as a secondary objective. There are three components of the reward function.

$$R(s, a, s') = \begin{cases} R_E & \text{if } s \in E \\ -d & \text{if } s \notin E, t \geq t_{end} \\ \log(P(a | s)) & \text{if } s \notin E, t < t_{end} \end{cases} \quad (1)$$

The first term of Equation 1 assigns a non-negative reward  $R_E$  if the path terminates and a failure event occurs. If the path terminates and an event does not occur, the second term of Equation 1 penalizes the learner by assigning the negative of the miss distance  $d$  to the learner. The miss distance is some measure defined by the user that depends on  $s$  and indicates how close the simulation came to a failure. If such a measure is not available, then  $-d$  can be set to a large negative constant. However, providing an appropriate miss distance can greatly accelerate the search by giving the learner the ability to distinguish the desirability of two paths that do not contain failure events. The third term of Equation 1 maximizes the overall path probability by awarding the log probability of

each transition. The transition probability is given by  $P(s' | s, a)P(a | s)$ . Since we have chosen our actions to deterministically set the stochastic variables of the simulator, the transitions then becomes deterministic, i.e.,  $P(s' | s, a) = 1$ , and the transition probability simplifies to  $P(a | s)$ . Recall that reinforcement learning maximizes the expected sum of rewards. By choosing a reward of the log probability at each step, the reinforcement learning algorithm then maximizes the sum of the log probabilities, which is equivalent to maximizing the product of the probabilities.

The MDP can be optimized using standard reinforcement learning algorithms (Sutton & Barto, 1998; Wiering & van Otterlo, 2012). Existing reinforcement learning algorithms such as Monte Carlo tree search (MCTS) (Kocsis & Szepesvári, 2006) and Q-Learning (Watkins & Dayan, 1992) can be applied to optimize the decision process and find the optimal path.

### 3.2 Partial Observability

The formulation described in the previous section requires access to the full state of the simulator. In some applications, some or all of the state variables may not be accessible. For example, black box components in the simulator, such as software binaries, can maintain state without exposing it externally. Incomplete state information leads to different states being aliased to the same observation, which can confuse the learner, hinder learning, and lead to poor optimization performance.

We introduce an abstraction that relaxes the need for the simulator to expose its state. Instead of explicitly representing and passing the state into and out of the simulator, we now assume that the simulator maintains state internally and the state is updated in-place. In other words, we have previously assumed that the simulator is stateless, but now we assume that the simulator is stateful. Furthermore, rather than explicitly choosing and passing values of the stochastic variables as the actions, we use a pseudorandom seed  $\bar{a}$  as a proxy. The simulator uses  $\bar{a}$  to seed an internal random process that draws a sample of the stochastic variables  $a$ . We assume that setting the seed makes the sampling process deterministic and sampling uniformly over all pseudorandom seeds returns the natural distribution of the stochastic models in the simulator.

**Seed-Action Simulator.** A *seed-action simulator*  $\bar{S}$  is a stateful simulator that uses a pseudorandom seed input to update its state in-place. The hidden state  $s$  is not exposed externally, making the simulator appear non-Markovian to external processes, such as the reinforcement learner. The simulator uses  $\bar{a}$  to draw a sample of the stochastic variables  $a$  and transition to the next state  $s'$ . The next state replaces the current state in-place. The simulator returns the transition probability  $p$  given by  $P(a | s)$ ; a Boolean indicating whether an event occurred  $e$ ; and the miss distance  $d$ . While the state cannot be observed or set, the simulator transitions are deterministic given the pseudorandom seed  $\bar{a}$ . This property allows a previously visited state to be revisited by replaying the sequence of pseudorandom seeds  $\bar{a}_0, \dots, \bar{a}_t$  that leads to it starting from the initial state. In other words, we can use the sequence of pseudorandom seeds as the state. We use  $s$  to denote the hidden state of the simulator and  $\bar{s}$  to denote the sequence of seeds that induces  $s$ .

The seed-action simulator  $\bar{S}$  exposes the following simulation control functions:

- **INITIALIZE( $\bar{S}$ )** resets the simulator  $\bar{S}$  to a deterministic initial state  $s_0$ . The simulation state is modified in-place.
- **STEP( $\bar{S}, \bar{a}$ )** advances the state of the simulator by pseudorandom sampling. First, the pseudorandom seed  $\bar{a}$  is used to set the state of the simulator's pseudorandom process. Second, a sample  $a$  of the stochastic variables in  $\bar{S}$  is drawn according to the natural distribution of the stochastic model. Third, the simulator transitions to the next state  $s'$  given the current state



$s$  and action  $a$ , and the hidden state  $s$  of the simulator is updated. The simulator returns the transition probability  $p$  given by  $P(a | s)$ ; whether an event occurred  $e$ ; and the miss distance  $d$ .

- $\text{IS}_{\text{TERMINAL}}(\bar{S})$  returns true if the current state of the simulator is terminal and false otherwise.

Figure 3 illustrates the AST framework under the pseudorandom seed abstraction, where the simulator has been replaced by a seed-action simulator  $\bar{S}$ , which maintains a hidden state. The seed input is used to draw a random action and state transition and the state is updated in-place. The simulator outputs the transition probability  $p$ , a Boolean indicating whether an event occurred  $e$ , and the miss distance  $d$ . The reward function translates the simulator outputs into a reward and the optimization algorithm learns from the reward to optimize over discrete pseudorandom seeds.

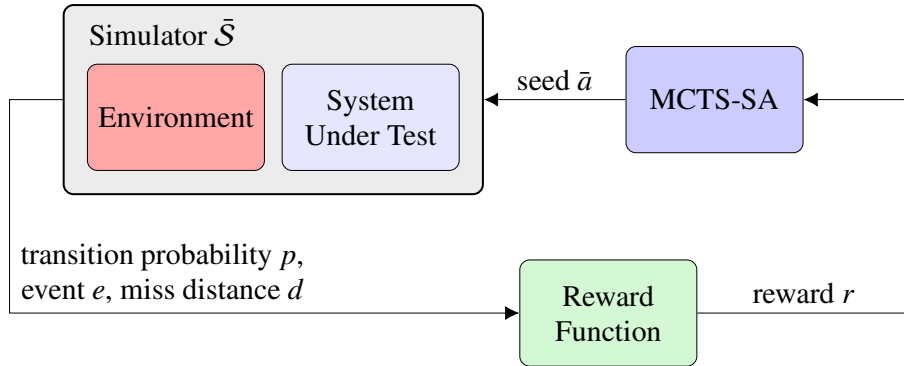


Figure 3: Adaptive stress testing of a partially observable system. We use a state-action simulator model where the simulator retains state, but does not expose it. The learner sets the pseudorandom seed that controls the pseudorandom number generator of the simulator making transitions deterministic. The simulator outputs the transition probability of the current transition, whether an event occurred, and a miss distance.

In addition to supporting hidden states, this abstraction also provides a very practical convenience. Large software simulators are often written in a distributed and modular fashion where each component maintains its own state. The simulator may consist of many of these components. Since the simulator state is the concatenation of the states of all the individual components, explicitly assembling and handling the state can break modularity and be a major implementation inconvenience. This abstraction, which uses in-place state update and pseudorandom seeds as a proxy to the actions, enables the simulator to maintain modularity of the components.

**MCTS-SA Algorithm.** We present Monte Carlo tree search for seed-action simulators (MCTS-SA). We base the algorithm on the double progressive widening variant of MCTS because the actions of the reinforcement learner are now pseudorandom seeds, which are vast (Couëtoux et al., 2011). The transition behavior of the simulator is deterministic given a pseudorandom seed input. Consequently, only a single next state is possible and there is no need to limit the number of next states. We simplify the algorithm by removing the progressive widening of the state and its associated parameters,  $k'$  and  $\alpha'$ . The action space is the space of all pseudorandom seeds. Since the seeds are discrete and do not have any semantic relationship, there is no need to distinguish between them. We choose the rollout policy and the action expansion function of MCTS to uniformly sample over all seeds. Sampling seeds uniformly generates unbiased samples of the next state from the simu-

lator. We use  $U_{seed}$  to denote the discrete uniform distribution over all possible seeds. The hidden state  $s$  of the simulator is not available to the reinforcement learner. However, since the simulator is deterministic given the pseudorandom seed input  $\bar{a}$ , we can revisit a previous state by replaying the sequence of seeds that leads to it starting from the initial state. As a result, we use the sequence of actions  $\bar{a}_0, \dots, \bar{a}_t$  as the state  $\bar{s}$  in the algorithm. The path with the highest total reward, that is, the sum of all the rewards received over the entire path, may, and likely will, be from a path that is encountered during a rollout. Since rollouts are not individually recorded, information about the best path can be lost. To ensure that the algorithm returns the best path seen over the entire search, we explicitly track the highest total reward seen,  $R^*$ , and the corresponding action sequence,  $\bar{s}^*$ .

The MCTS-SA algorithm is shown in Algorithm 1. The algorithm consists of a main loop that repeatedly performs forward simulations of the system while building the search tree and updating the state-action value estimates. The search tree  $\mathcal{T}$  is initially empty. Each simulation runs from initial state to terminal state. The path is determined by the sequence of pseudorandom seeds chosen by the algorithm, which falls into three stages for each simulation:

- *Search.* In the search stage, which is implemented by SIMULATE (line 13), the algorithm starts at the root of the tree and recursively selects a child to follow. At each visited state node, the progressive widening criteria (line 22) determines whether to choose amongst existing actions (seeds) or to expand the number of children by sampling a new action. The criterion limits the number of actions at a state  $s$  to be no more than polynomial in the total number of visits to that state. Specifically, a new action  $\bar{a}$  is sampled from a discrete uniform distribution over all seeds  $U_{seed}$  if  $\|A(\bar{s})\| < kN(\bar{s})^\alpha$ , where  $k$  and  $\alpha$  are parameters,  $\|A(\bar{s})\|$  is the number of previously visited actions at state  $\bar{s}$ , and  $N(\bar{s})$  is the total number of visits to state  $\bar{s}$ . Otherwise, the existing action that maximizes

$$Q(\bar{s}, \bar{a}) + c \sqrt{\frac{\log N(\bar{s})}{N(\bar{s}, \bar{a})}} \quad (2)$$

is chosen (line 27), where  $c$  is a parameter that controls the amount of exploration in the search, and  $N(\bar{s}, \bar{a})$  is the total number of visits to action  $\bar{a}$  in state  $\bar{s}$ . Equation 2 is the upper confidence tree (UCT) equation (Kocsis & Szepesvári, 2006). The second term in the equation is an *exploration bonus* that encourages selecting actions that have not been tried as frequently. The action is used to advance the simulator to the next state and the reward is evaluated. The search stage continues in this manner until the system transitions to a state that is not in the tree.

- *Expansion.* Once we have reached a state that is not in the tree  $\mathcal{T}$ , we create a new node for the state and add it (line 18). The set of previously taken actions from this state,  $A(\bar{s})$ , is initially empty and the number of visits to this state  $N(\bar{s})$  is initialized to zero.
- *Rollout.* Starting from the state created in the expansion stage, we perform a *rollout* that repeatedly samples state transitions until the desired termination is reached (line 20). In the ROLLOUT function (line 36), state transitions are drawn from the simulator with actions chosen according to a rollout policy, which we set as the discrete uniform distribution over all seeds  $U_{seed}$ .

At each step in the simulation, the reward function is evaluated and the reward is used to update estimates of the state-action values  $Q(\bar{s}, \bar{a})$  (line 34). The values are used to direct the search. At the end of each simulation, the best total reward  $R^*$  and best path  $\bar{s}^*$  are updated (lines 10–11).

**Algorithm 1** MCTS for seed-action simulators

---

```

1: ▶ Inputs: Seed-action simulator  $\bar{\mathcal{S}}$ 
2: ▶ Returns: Sequence of seeds that induces path with highest total reward  $\bar{s}^*$ 
3: function MCTS( $\bar{\mathcal{S}}$ )
4:   global  $\bar{s}_T \leftarrow \emptyset$ 
5:    $(\bar{s}^*, R^*) \leftarrow (\emptyset, -\infty)$ 
6:   loop
7:      $\bar{s} \leftarrow \emptyset$ 
8:     INITIALIZE( $\bar{\mathcal{S}}$ )
9:      $R_{total} \leftarrow \text{SIMULATE}(\bar{\mathcal{S}}, \bar{s})$ 
10:    if  $R_{total} > R^*$ 
11:       $(\bar{s}^*, R^*) \leftarrow (\bar{s}_T, R_{total})$ 
12:    return  $\bar{s}^*$ 
13: function SIMULATE( $\bar{\mathcal{S}}, \bar{s}$ )
14:   if ISTERMINAL( $\bar{\mathcal{S}}$ )
15:      $\bar{s}_T \leftarrow \bar{s}$ 
16:     return 0
17:   if  $\bar{s} \notin \mathcal{T}$ 
18:      $\mathcal{T} \leftarrow \mathcal{T} \cup \{\bar{s}\}$ 
19:      $(N(\bar{s}), A(\bar{s})) \leftarrow (0, \emptyset)$ 
20:     return ROLLOUT( $\bar{\mathcal{S}}, \bar{s}$ )
21:    $N(\bar{s}) \leftarrow N(\bar{s}) + 1$ 
22:   if  $\|N(\bar{s}, \bar{a})\| < kN(\bar{s})^\alpha$ 
23:      $\bar{a} \sim U_{seed}$ 
24:      $(N(\bar{s}, \bar{a}), V(\bar{s}, \bar{a})) \leftarrow (0, \emptyset)$ 
25:      $Q(\bar{s}, \bar{a}) \leftarrow 0$ 
26:      $A(\bar{s}) \leftarrow A(\bar{s}) \cup \{\bar{a}\}$ 
27:      $\bar{a} \leftarrow \operatorname{argmax}_a Q(\bar{s}, a) + c \sqrt{\frac{\log N(\bar{s})}{N(\bar{s}, a)}}$ 
28:      $(p, e, d) \leftarrow \text{STEP}(\bar{\mathcal{S}}, \bar{a})$ 
29:      $\tau \leftarrow \text{ISTERMINAL}(\bar{\mathcal{S}})$ 
30:      $r \leftarrow \text{REWARD}(p, e, d, \tau)$ 
31:      $\bar{s}' \leftarrow [\bar{s}, \bar{a}]$ 
32:      $q \leftarrow r + \text{SIMULATE}(\bar{\mathcal{S}}, \bar{s}')$ 
33:      $N(\bar{s}, \bar{a}) \leftarrow N(\bar{s}, \bar{a}) + 1$ 
34:      $Q(\bar{s}, \bar{a}) \leftarrow Q(\bar{s}, \bar{a}) + \frac{q - Q(\bar{s}, \bar{a})}{N(\bar{s}, \bar{a})}$ 
35:     return  $q$ 
36: function ROLLOUT( $\bar{\mathcal{S}}, \bar{s}$ )
37:   if ISTERMINAL( $\bar{\mathcal{S}}$ )
38:      $\bar{s}_T \leftarrow \bar{s}$ 
39:     return 0
40:    $\bar{a} \sim U_{seed}$ 
41:    $(p, e, d) \leftarrow \text{STEP}(\bar{\mathcal{S}}, \bar{a})$ 
42:    $\tau \leftarrow \text{ISTERMINAL}(\bar{\mathcal{S}})$ 
43:    $r \leftarrow \text{REWARD}(p, e, d, \tau)$ 
44:    $\bar{s}' \leftarrow [\bar{s}, \bar{a}]$ 
45:   return  $r + \text{ROLLOUT}(\bar{\mathcal{S}}, \bar{s}')$ 

```

---

Simulations are run until the stopping criterion is met. The criterion is a fixed number of iterations for all our experiments except for the performance study where we used a fixed computational budget. The algorithm returns the path with the highest total reward represented as a sequence of pseudorandom seeds. The sequence of seeds can be used to replay the simulator to reproduce the failure events.

**Reward Function.** The reward function for AST for state-action simulator is given in Equation 3. The reward is expressed as a function of state-action simulator outputs and a Boolean variable  $\tau$  which indicates whether the simulator has terminated, i.e.,  $\tau = \text{IsTERMINAL}(\bar{S})$ . The three components mirror those in Equation 1. The indicator function  $\mathbb{1}\{x\}$  returns 1 if  $x$  is true and 0 otherwise.

$$\begin{aligned} R(p, e, d, \tau) = & + R_E \cdot \mathbb{1}\{e\} \\ & - d \cdot \mathbb{1}\{-e \wedge \tau\} \\ & \log p \cdot \mathbb{1}\{-e \wedge \neg\tau\} \end{aligned} \quad (3)$$

**Computational Complexity.** Each iteration of the MCTS main loop simulates a path from initial state to terminal state. As a result, the number of calls to the simulator is linear in the number of loop iterations. The computation time thus varies as  $O(N_{loop} \cdot (T_{\text{INITIALIZE}} + N_{steps} \cdot T_{\text{STEP}}))$ , where  $N_{loop}$  is the number of loop iterations,  $T_{\text{INITIALIZE}}$  is the computation time of INITIALIZE,  $N_{steps}$  is the average number of steps in the simulation, and  $T_{\text{STEP}}$  is the computation time of the STEP function.

#### 4. Differential Adaptive Stress Testing

The previous section presented AST, which can be used to find the most likely failure path in a system. In some applications, we may not be so interested in finding failures in absolute terms, but relative to some comparable baseline system. For example, in regression testing, we may be interested in seeing whether a new version of a software has introduced bugs that were not there before. This section presents differential adaptive stress testing (DAST), a stress testing method for efficiently finding the most likely path to a failure event that occurs in the system under test, but not in the baseline. The key idea behind DAST is to drive two simulators in parallel and maximize the difference in their outcomes. Following the AST approach, DAST formulates stress testing as a sequential decision-making problem and optimizes it using reinforcement learning. We use the MCTS-SA algorithm described in Algorithm 1 for optimization, which is appropriate for partially observable systems.

Figure 4 illustrates the DAST framework. We create two instances of the simulator  $\bar{S}^{(1)}$  and  $\bar{S}^{(2)}$ . The instances are identical except that  $\bar{S}^{(1)}$  contains the system under test, while  $\bar{S}^{(2)}$  contains the baseline system. In particular, they contain identical models of the environment with which the test systems interface. The simulators are driven by the same pseudorandom seed input, which leads to the same sequence of stochastic variables being drawn from the environment when the behaviors of the test and baseline systems match. When the behavior of the two systems diverge, the seed automatically allows different stochastic variables to be drawn from each simulator following their diverging states. We define a combined simulator that contains the two parallel simulators  $\bar{S}^{(1)}$  and  $\bar{S}^{(2)}$ . They are both driven by the same input seed  $\bar{a}$ . Each simulator produces its own set of outputs, which include the transition probability  $p$ , an indicator of whether an event occurred  $e$ , and the miss

distance  $d$ . These variables are combined in a reward function, where a single reward is provided to the reinforcement learner. Finally, the MCTS-SA algorithm chooses seeds to maximize the reward it receives. The superscripts on the variables  $p, e, d$  and  $\tau$  indicate the associated simulator.

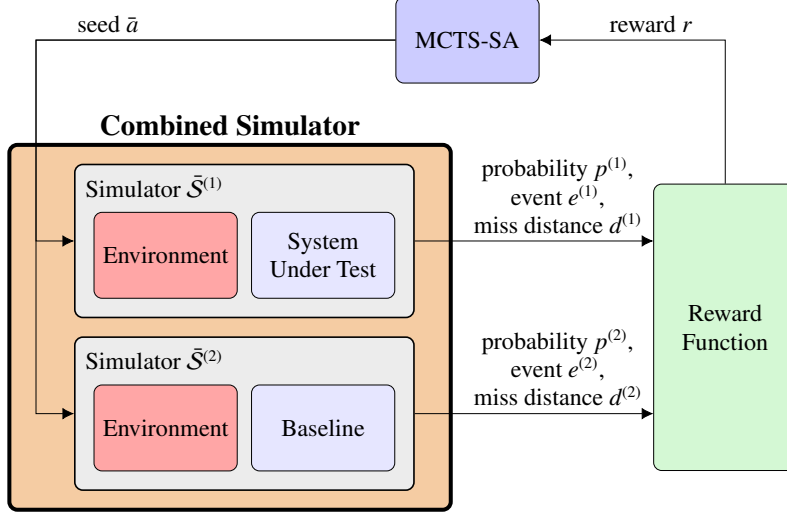


Figure 4: Differential adaptive stress testing framework. Two parallel simulators, one running the system under test and one running the baseline, are searched simultaneously. The search drives one simulator to failure while keeping the second simulator away from one.

**Reward Function.** The reward function combines the output from the two individual simulators to produce a single reward for the learner. The primary objective of the reward function is to maximize the difference in outcomes of the simulators driving the first simulator to a failure event, while keeping the second simulator away from one. The secondary objective is to maximize the path probabilities of the two simulators to produce the most likely paths. The DAST reward function is given by Equation 4. The indicator function  $\mathbb{1}\{x\}$  returns 1 if  $x$  is true and 0 otherwise.

$$\begin{aligned}
 R(p^{(1)}, e^{(1)}, d^{(1)}, \tau^{(1)}, p^{(2)}, e^{(2)}, d^{(2)}, \tau^{(2)}) = & + R_E \cdot \mathbb{1}\{e^{(1)}\} \\
 & - d^{(1)} \cdot \mathbb{1}\{\neg e^{(1)} \wedge \tau^{(1)}\} \\
 & - R_E \cdot \mathbb{1}\{e^{(2)}\} \\
 & + d^{(2)} \cdot \mathbb{1}\{\neg e^{(2)} \wedge \tau^{(2)}\} \\
 & + (\log p^{(1)} + \log p^{(2)}) \cdot \mathbb{1}\{\neg e^{(1)} \wedge \neg e^{(2)} \wedge \neg \tau\} \quad (4)
 \end{aligned}$$

The DAST reward function extends the AST reward function to the differential setting and has a similar structure. The first term gives a non-negative reward  $R_E$  to the learner if the first simulator  $\bar{S}^{(1)}$  terminates in an event. If  $\bar{S}^{(1)}$  terminates and an event did not occur, then the second term penalizes the learner by giving the negative miss distance  $-d^{(1)}$ . The third and fourth terms are the negations of the first and second terms, respectively, applied to the second simulator  $\bar{S}^{(2)}$ . The third term gives  $-R_E$  if  $\bar{S}^{(2)}$  terminates in an event and the fourth term gives  $d^{(2)}$  if  $\bar{S}^{(2)}$  terminates and an event did not occur. To maximize the probabilities of the paths, the fifth term gives the sum of the log transition probabilities of both simulators. The terminal state of the simulators are

treated as *absorbing*. That is, once a simulator enters a terminal state, it stays there for all subsequent transitions and collects zero reward for these transitions. The Boolean variables  $\tau^{(1)}$  and  $\tau^{(2)}$  indicate whether  $\bar{S}^{(1)}$  and  $\bar{S}^{(2)}$  have terminated, respectively. The combined simulator terminates when both simulators have terminated, i.e.,  $\tau = \text{IS\_TERMINAL}(\bar{S}) = \tau^{(1)} \wedge \tau^{(2)}$ .

We optimize the reward function using the same MCTS-SA algorithm described in Algorithm 1 as used in AST, which applies to partially observable systems. Because the algorithm is based on scalar rewards and pseudorandom seeds, the internal details of the simulator are abstracted from the reinforcement learner. As a result, no modifications to the algorithm are necessary.

## 5. Aircraft Collision Avoidance Application

Aircraft collision avoidance systems are mandated on all large transport and cargo aircraft in the United States to help prevent mid-air collisions. Its operation has played a crucial role in the exceptional level of safety in the national airspace (Kuchar & Drumm, 2007). The Traffic Alert and Collision Avoidance System (TCAS) is currently deployed in the United States and many countries around the world. TCAS has been very successful at protecting aircraft from mid-air collisions. However, studies have revealed fundamental limitations in TCAS that prevent it from operating effectively in the next-generation airspace (Kuchar & Drumm, 2007). To address the growing needs of the national airspace, the Federal Aviation Administration (FAA) has decided to create a new aircraft collision avoidance system. The next-generation Airborne Collision Avoidance System (ACAS X) is currently being developed and tested and promises a number of improvements over TCAS including a reduction in collision risk while simultaneously reducing the number of unnecessary alerts (Kochenderfer et al., 2012).

ACAS X has been shown to be much more operationally suitable than TCAS (Federal Aviation Administration, 2018). Table 1 is a comparison of ACAS X and TCAS on several key operational metrics evaluated on a number of simulated aircraft encounter datasets. The data is excerpted from the results of many studies performed at MIT Lincoln Laboratory (MIT-LL) and presented at the RTCA (Federal Aviation Administration, 2018). ACAS X shows significant improvements in overall safety and alert rates compared to TCAS. The primary metric of safety is the probability of a near mid-air collision (NMAC),  $P_{NMAC}$ . An NMAC is defined as two aircraft coming closer than 500 feet horizontally and 100 feet vertically. On large encounter datasets, ACAS X is shown to reduce the probability of NMAC by 17% to 54% compared to TCAS. Alert metrics show significant improvements over TCAS as well, including the aggregate alert rate, which is the number of times the collision avoidance system alerts (counted by aircraft); and the 500 feet corrective alert rate, which is the number of alerts issued in encounters where the aircraft are flying level and vertically separated by exactly 500 feet. ACAS X also significantly improves metrics on generally undesirable scenarios such as the altitude crossing rate, which is the number of encounters where two aircraft cross in altitude; and the reversal rate, which is the number of times the collision avoidance system first advises the pilot to maneuver in one direction, then later advises the pilot to maneuver in the opposite direction.

Studies have shown that the risk of NMAC is extremely small and moreover ACAS X reduces the risk even further over TCAS overall. However, the risk of NMAC cannot be completely eliminated due to factors such as surveillance noise, pilot response delay, and the need for an acceptable alert rate (Kochenderfer et al., 2012). Because NMACs are such important safety events, it is important to study and understand the rare circumstances under which they can still occur even if they

Table 1: A comparison of ACAS X and TCAS operational metrics on various encounter datasets. The data is excerpted from (Federal Aviation Administration, 2018). ACAS X significantly improves overall safety, alert rates, and other operational metrics compared to TCAS.

Metric	Dataset	Number of encounters	TCAS v7.1	ACAS Xa 0.10.3	Improvement over TCAS
Safety ( $P_{NMAC}$ )	LLCEM	5,956,128	$2.179 \cdot 10^{-4}$	$1.744 \cdot 10^{-4}$	19.57%
Safety ( $P_{NMAC}$ )	SAVAL	75,173,906	$4.361 \cdot 10^{-4}$	$3.627 \cdot 10^{-4}$	16.82%
Safety ( $P_{NMAC}$ )	SA01	100,000	$4.106 \cdot 10^{-2}$	$1.873 \cdot 10^{-2}$	54.37%
Alert Rate (by aircraft)	TRAMS	293,101	252,656	121,267	52.00%
500' Corrective Alert Rate	TRAMS	175,184	14,912	9,919	33.48%
Altitude Crossing Rate	TRAMS	293,101	3,196	1,582	50.5%
Reversal Rate	TRAMS	293,101	1,029	556	45.97%

are extremely unlikely. Understanding the nature of the residual NMAC risk is important for certification and to inform the development of future iterations of the system. This paper uses AST and DAST to find and analyze the rare corner cases where an NMAC can still occur.

## 5.1 ACAS X Operation

There are several versions of ACAS X under development. This paper considers a development (and not final) version of ACAS Xa, which uses active surveillance and is designed to be a direct replacement to TCAS. Despite the internal logics of ACAS X and TCAS being derived completely differently, the input and output interfaces of these two systems are identical. As a result, the following description of aircraft collision avoidance systems applies to both ACAS X and TCAS.

Airborne collision avoidance systems monitor the airspace around an aircraft and issue alerts to the pilot if a conflict with another aircraft is detected. These alerts, called resolution advisories (RAs), instruct the pilot to maneuver the aircraft to a certain target vertical velocity and maintain it. The advisories are typically issued when the aircraft are within approximately 20-40 seconds to a potential collision. Table 2 lists the possible primary RAs. We use  $\dot{z}_{own}$  to denote the current vertical velocity of own aircraft.

Table 2: Primary ACAS X advisories

Abbreviation	Description	Rate to Maintain (ft/min)
COC	clear of conflict	N/A
DND	do not descend	0
DNC	do not climb	0
MAINTAIN	maintain current rate	$\dot{z}_{own}$
DS1500	descend at 1,500 ft/min	-1500
CL1500	climb at 1,500 ft/min	+1500
DS2500	descend at 2,500 ft/min	-2500
CL2500	climb at 2,500 ft/min	+2500

The COC advisory stands for “clear of conflict” and is equivalent to no advisory. The pilot is free to choose how to control the aircraft. The DND and DNC advisories stand for “do not descend” and “do not climb”, respectively. They restrict the pilot from flying in a certain direction. The MAINTAIN advisory is preventative and instructs the pilot to maintain the current vertical rate of the aircraft. The advisories DS1500 and CL1500 instruct the pilot to descend or climb at 1,500 feet per minute. The pilot is expected to maneuver the aircraft at  $\frac{1}{4}g$  acceleration until the target vertical rate is reached then maintain that vertical rate. The DS2500 and CL2500 advisories instruct the pilot to descend or climb at an increased rate of 2,500 feet per minute. These advisories are strengthened advisories and expect a stronger response from the pilot. For these strengthened RAs, the pilot is expected to maneuver at  $\frac{1}{3}g$  acceleration until the target vertical rate is reached then maintain that vertical rate. Strengthened RAs must follow a weaker RA of the same vertical direction. They cannot be issued directly. For example, a CL1500 advisory must precede a CL2500 advisory. Advisories issued by collision avoidance systems on different aircraft are not completely independent. When an RA is issued, a coordination message is broadcasted to other nearby aircraft to prevent other collision avoidance systems from accidentally issuing an RA in the same vertical direction.

## 5.2 Experimental Setup

We construct a seed-action simulator modeling an aircraft mid-air encounter. The overall architecture of the simulator for two aircraft is shown in Figure 5. Simulation models capture the key aspects of the encounter, including the initial state, sensors, collision avoidance system, pilot response, and aircraft dynamics.

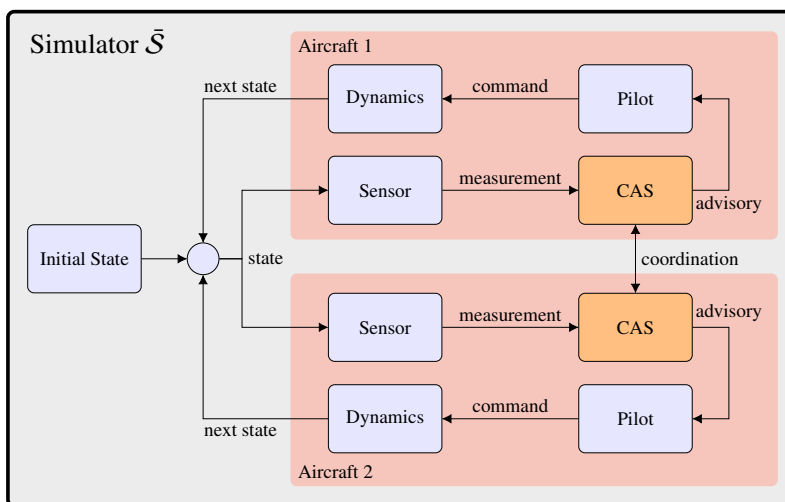


Figure 5: System diagram for pairwise encounters. Two aircraft simulation loops are used. Simulation models sensors, collision avoidance system, pilot response, aircraft dynamics, and their interactions.



### 5.2.1 SIMULATION MODEL

**Initial State.** The initial state of the encounter includes initial positions, velocities, and headings of the aircraft. The initial state is drawn from a distribution that gives realistic initial configurations of aircraft that are likely to lead to NMAC. Once the initial state is sampled, it is fixed for the duration of the search. In our experiments, pairwise (two-aircraft) encounters are initialized using the Lincoln Laboratory Correlated Aircraft Encounter Model (LLCEM) (Kochenderfer, Espindle, Kuchar, & Griffith, 2008; Kochenderfer, Edwards, Espindle, Kuchar, & Griffith, 2010). LLCEM is a statistical model learned from a large body of radar data of the entire national airspace. We follow the encounter generation procedure described in the paper (Kochenderfer et al., 2008). Multi-threat (three-aircraft) encounters use the *Star model*, which initializes aircraft on a circle heading towards the origin spaced apart at equal angles. Initial airspeed, altitude, and vertical rate are sampled from a uniform distribution over a prespecified range. The horizontal distance from the origin is set such that without intervention, the aircraft intersect at approximately 40 seconds into the encounter.

**Sensor Model.** The sensor model captures how the collision avoidance system perceives the world. We assume active, beacon-based radar capability with no noise. For own aircraft, the sensor measures the vertical rate, barometric altitude, heading, and height above ground. For each intruding aircraft, the sensor measures slant range (relative distance to intruder), bearing (relative horizontal angle to intruder), and relative altitude.

**Collision Avoidance System.** The collision avoidance system is the system under test. We use a prototype of ACAS X in the form of a binary library obtained from the FAA. The binary has a minimal interface that allows initializing and stepping the state forward in time. The system maintains internal state, but does not expose it. The primary output of the ACAS X system is the RA. ACAS X has a coordination mechanism to ensure that issued RAs from different aircraft are compatible with one another, i.e., that two aircraft are not instructed to maneuver in the same vertical direction. The messages are communicated to all nearby aircraft through coordination messages. Our differential studies use TCAS as a baseline. Our implementation of TCAS is also a binary library obtained from the FAA. Both binaries have identical input and output interfaces making them interchangeable in the simulator.

**Pilot Model.** The pilot model consists of a model for the pilot's intent and a model for how the pilot responds to an RA. The pilot's intent is how the pilot would fly the aircraft if there are no RAs. To model intended commands, we use the pilot command model in LLCEM, which gives a realistic stochastic model of aircraft commands in the airspace (Kochenderfer et al., 2008). The pilot response model defines how pilots respond to an issued RA. Pilots are assumed to respond deterministically to an RA with perfect compliance after a fixed delay (International Civil Aviation Organization, 2007). Pilots respond to initial RAs with a five-second delay and subsequent RAs (i.e., strengthenings and reversals) with a three-second delay. During the initial delay period, the pilot continues to fly the intended trajectory. During response delays from subsequent RAs, the pilot continues responding to the previous RA. Multiple RAs issued successively are queued so that both their order and timing are preserved. In the case where a subsequent RA is issued within 2 seconds or less of an initial RA, the timing of the subsequent RA is used and the initial RA is skipped. The pilot command includes commanded airspeed acceleration, commanded vertical rate, and commanded turn rate.

**Aircraft Dynamics Model.** The aircraft dynamics model determines how the state of the aircraft propagates with time. The aircraft state includes the airspeed, position north, position east,

altitude, roll angle, pitch angle, and heading angle. The aircraft state is propagated forward at 1 Hz using forward Euler integration.

In our experiments, the commands of the pilots when not responding to an advisory are stochastic and are being optimized by the algorithm. When no RA is active, the pilot commands follow the stochastic dynamic model of LLCCEM. When an RA is active, the vertical component of the pilot’s command follows the pilot response model, while the other components follow LLCCEM. Other simulation components are deterministic in our experiments. However, in the future, we may consider stochastic models for sensors, aircraft dynamics, and pilot response.

### 5.2.2 REWARD FUNCTION

We use the reward function defined in Equation 3 for optimization. The event space  $E$  is defined to be an NMAC, which occurs when two aircraft are closer than 100 feet vertically and 500 feet horizontally. We define the miss distance  $d$  to be the distance of closest approach, which is the Euclidean distance of the aircraft at their closest point in the encounter. The distance of closest approach is a good metric because it is monotonically decreasing as trajectories get closer and reach a minimum at an NMAC. Because the models in the simulator use continuous distributions, we use the transition probability density in the reward function.

### 5.3 Stress Testing Single-Threat Encounters

We apply AST to analyze NMACs in encounters involving two aircraft. We searched 100 encounters initialized using samples from LLCCEM. The configuration is shown in Table 3. Of the 100 encounters searched, 18 encounters contained an NMAC, yielding an empirical find rate of 18%. When the optimization algorithm completes, it returns the path with the highest reward regardless of whether the path contains an NMAC. When the returned path does not contain an NMAC, it is uncertain whether an NMAC exists and the algorithm was unable to find it, or whether no NMAC is reachable given the initial state of the encounter. We manually cluster the NMAC encounters and present our findings.

Table 3: Single-threat configuration

Simulation	
number of aircraft	2
initialization	LLCEM
sensors	active, beacon-based, noiseless
collision avoidance system	ACAS Xa Run 13 libcas 0.8.5
pilot response model	deterministic 5s–3s
MCTS	
maximum steps	50
iterations	2000
exploration constant	100.0
$k$	0.5
$\alpha$	0.85

**Crossing Time.** We observed a number of NMACs resulting from well-timed vertical maneuvers. In particular, several encounters included aircraft crossing in altitude during the delay period of an initial RA. Figure 6 shows one such encounter that eventually ends in an NMAC at 36 seconds into the encounter. The probability density of the encounter evaluated under LLCCEM is  $5.3 \cdot 10^{-18}$ . This measure can be used as an unnormalized measure of likelihood of occurrence. In this encounter, the aircraft cross in altitude during pilot 1’s delay period. The crossing leads to aircraft 1 starting the climb from below aircraft 2. The subsequent reversal later in the encounter is unable to resolve the conflict due to the pilot response delay.

NMAC encounter plots contain horizontal tracks (top-down view) and vertical profile (altitude versus time). Aircraft numbers are indicated at the start and end of each trajectory. RA codes are labeled at the time of occurrence. Marker colors indicate the RA issued: blue for COC, orange for CL1500, red for CL2500, cyan for DS1500, purple for DS2500, and grey for DNC/DND/MAINTAIN/MULTITHREAT. Symbols inside the markers indicate the state of the pilot response: no symbol for not responding, dash for responding to previous RA, and asterisk for responding to current RA.

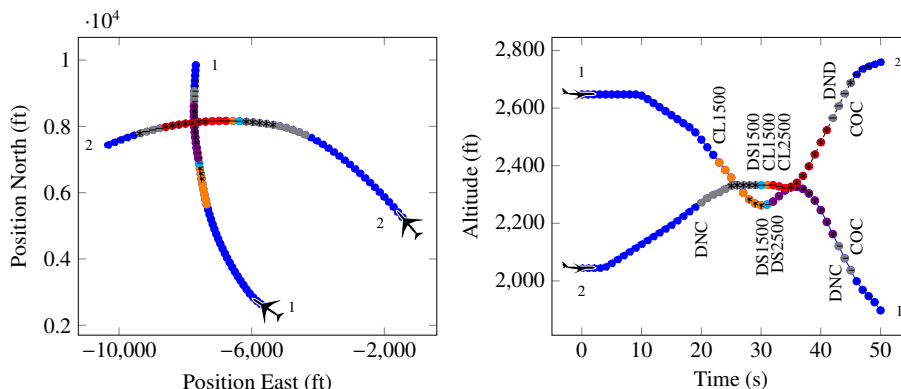


Figure 6: NMAC encounter where the aircraft cross in altitude during pilot delay. The aircraft cross in altitude after aircraft 1’s RA has been issued, but before they start to respond. The aircraft starts to climb from below the intruder and the encounter ends in an NMAC at 36 seconds.

**High Turn and Vertical Rates.** Turns at high rates quickly shorten the time to closest approach. ACAS X does not have full state information about its intruder and must estimate it by tracking relative distance, relative angle, and the intruder altitude. Figure 7 shows an example of an encounter that has similar crossing behavior as Figure 6 but exacerbated by the high turn rate of aircraft 2 (approximately 1.5 times the standard turn rate). In this scenario, the aircraft become almost head-on at the time of closest approach and a reversal is not attempted. An NMAC with a probability density of  $6.5 \cdot 10^{-17}$  occurs at 48 seconds into the encounter. Aircraft 1 is also coincidentally descending at a high vertical rate. The combination makes this encounter operationally very unlikely.

**Maneuvering Against RA.** Our analysis revealed a number of NMAC encounters where the pilot initially maneuvers against the issued RA before complying. That is, after the pilot receives the RA, they maneuver the aircraft in the opposite direction of what is instructed by the RA for the duration of the pilot response delay before subsequently complying and reversing direction. Pilots do not normally maneuver in this manner and so this scenario represents a very operationally rare

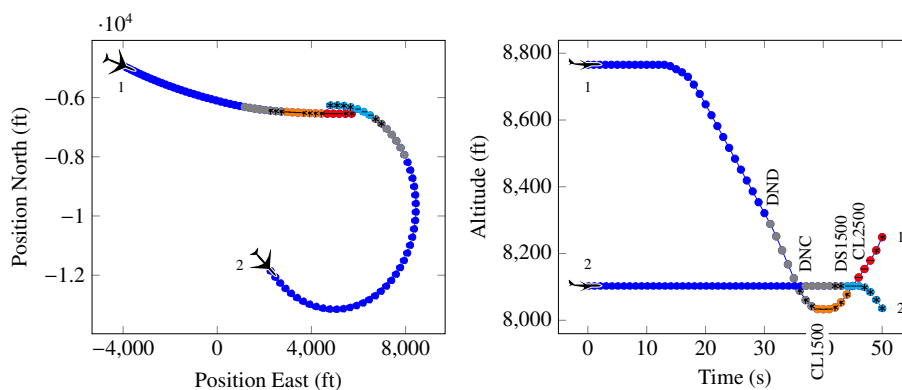


Figure 7: NMAC encounter where one aircraft is turning at high rate while the other is descending at high vertical rate. The encounter ends in an NMAC, but the combination is operationally very rare.

case. Even so, ACAS X does seem to be able to resolve the majority of these initially disobeying cases. In most cases, the maneuvering must be very aggressive against the RA to result in an NMAC.

**Sudden Aggressive Maneuvering.** Sudden maneuvers can lead to NMACs when they are sufficiently aggressive. In particular, we observed some NMAC encounters where two aircraft are approaching one another separated in altitude and flying level, then one aircraft suddenly accelerates vertically towards the other aircraft as they are about to pass. Under these circumstances, given the pilot response delays and dynamic limits of the aircraft, there is insufficient time and distance remaining for the collision avoidance system to resolve the conflict. Pilots do not normally fly so aggressively in operation, so this case is extremely unlikely. In fact, they are even more rare than our model predicts. ACAS X issues traffic alerts (TAs) to alert pilots to nearby traffic, so that pilots are made aware of intruding aircraft well before the initial RA. These advance warnings increase the pilot’s situational awareness and reduce blunders like these. Our simulator does not model the effect of TAs. One course of action would be for ACAS X to intervene preemptively. While this reduces the risk of possible sudden behavior, it also increases the alert rate of the system. Ultimately the designer must assess the probabilities of various scenarios and find the delicate balance between risk of collision and issuing too many advisories. Since these scenarios are extremely rare, we must trade off accordingly.

**Combined Factors.** In our experiments, it is rare for an NMAC to be attributable to a single cause. More commonly, a combination of factors contribute to the NMAC. Figure 6 shows an example of such an encounter. Although crossing time played a crucial role, there are a number of other factors that are important. The horizontal behavior where they are turning into each other is significant as it reduces the time to closest approach. The two vertical maneuvers of aircraft 1 before receiving an RA are also important. Similar observations can be made on many of the other NMAC encounters found.

#### 5.4 Stress Testing Multi-Threat Encounters

We applied AST to analyze NMACs in three-aircraft encounters. We searched 100 encounters initialized using samples from the Star model. The configuration is shown in Table 4. We found 25 NMACs out of 100 encounters searched, yielding a find rate of 25%.

Table 4: Multi-threat configuration

Simulation	
number of aircraft	3
initialization	Star model
sensors	active, beacon-based, noiseless
collision avoidance system	ACAS Xa Run 13 libcas 0.8.5
pilot response model	deterministic 5s–3s
MCTS	
maximum steps	50
iterations	1000
exploration constant	100.0
$k$	0.5
$\alpha$	0.85

**Pairwise Coordination in Multi-Threat.** Our algorithm discovered a number of NMAC encounters where all aircraft are issued a “multi-threat” RA and asked to follow an identical climb rate. Complying with the RA results in the aircraft closing horizontally without gaining vertical separation. Figure 8 shows an example of such an encounter where an NMAC occurs with probability density  $5.8 \cdot 10^{-7}$  at 38 seconds into the encounter. In discussing these results with the ACAS X development team, we learned that this behavior is a known issue that can arise when performing multi-aircraft coordination using a pairwise coordination mechanism. The pairwise coordination messages in essence determine which aircraft will climb and which will descend in an encounter. Since coordination messaging occurs pairwise, under rare circumstances it is possible for each aircraft to receive conflicting coordination messages from the other aircraft in the scenario. In nominal encounters, the aircraft that receives conflicting coordination messages from two aircraft remains level and lets the other aircraft climb or descend around it. However, in these encounters, all three aircraft receive conflicting coordination messages. Although very rare, this is an important case that is being addressed by both TCAS and ACAS X development teams.

**Limited Maneuverable Space.** In general, multi-threat encounters are more challenging to resolve than pairwise encounters because there is less open space for the aircraft to maneuver. Figure 9 shows an example of an NMAC encounter where aircraft 1 (the aircraft in the middle altitude between 10 and 36 seconds) needs to simultaneously avoid an aircraft below and a vertically closing aircraft from above. An NMAC with a probability density of  $1.0 \cdot 10^{-16}$  occurs at 39 seconds into the encounter. Aircraft 2’s downward maneuver greatly reduces the maneuverable airspace of aircraft 1. These encounters are undoubtedly extremely challenging for a collision avoidance system and it is unclear whether any satisfactory resolution exists. Nevertheless, we gain insight by observing how the collision avoidance system behaves under such circumstances. A future version of ACAS X will add horizontal advisories in addition to vertical ones, which will help in such encounters by adding an additional dimension controllable by the collision avoidance system.

**Pairwise Phenomena.** Phenomena that appear in pairwise encounters also appear in multi-threat encounters. The presence of the third aircraft typically exacerbates the encounter. In our multi-threat analysis, we noted similar phenomena related to crossing time, maneuvering against

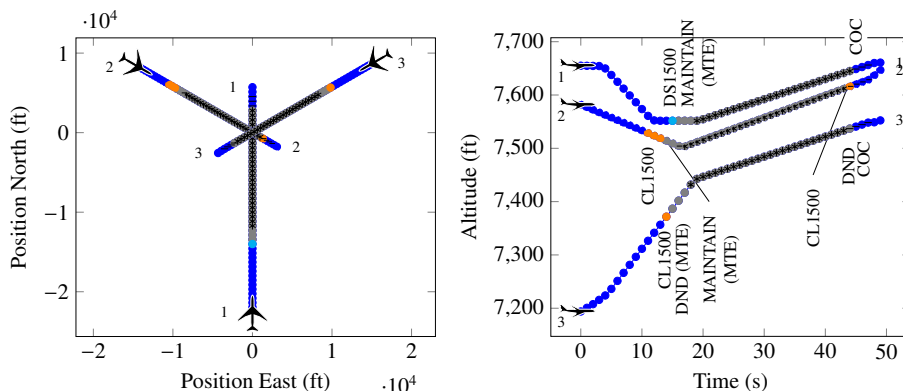


Figure 8: NMAC encounter where all aircraft receive pairwise conflicting coordination messages and do not maneuver. The encounter ends in an NMAC at 38 seconds. This is a very rare but important case that the ACAS X team is addressing.

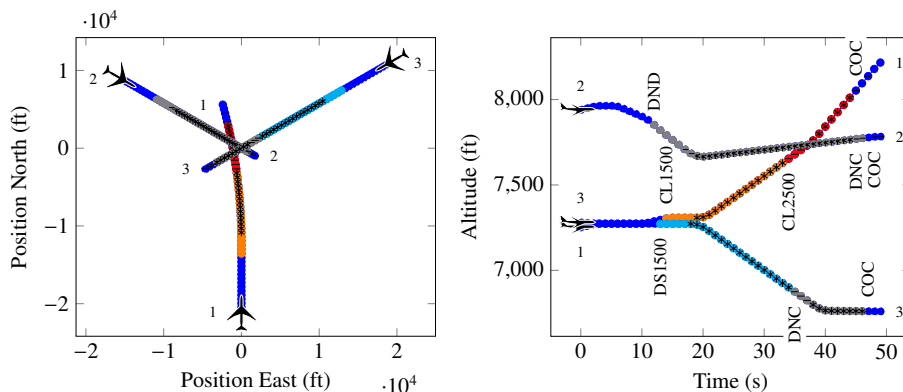


Figure 9: NMAC encounter where the aircraft have limited maneuverable airspace. Aircraft 1 tries to avoid aircraft 2 while maneuvering away from aircraft 3. The encounter ends in an NMAC at 39 seconds.

RA, and sudden aggressive maneuvering as discussed previously. We did not observe any cases related to high turn rates in the multi-threat setting due to our use of the Star model.

**5.5 Stress Testing ACAS X Relative to TCAS Baseline**

We apply DAST to perform differential stress testing of ACAS X relative to a TCAS baseline. We seek to find NMAC encounters that occur in ACAS X but not in TCAS. The search is extremely difficult. Not only are both ACAS X and TCAS systems extremely safe, which means that NMACs are extremely rare, but also ACAS X is a much safer system than TCAS overall, which makes cases where ACAS X has NMAC but TCAS does not extremely rare. We seek to find those extremely rare corner cases.

We searched 2700 pairwise encounters initialized with samples from LLCEM. The configuration is shown in Table 5. The top 10 highest reward paths were returned for each encounter initialization producing a total of 27,000 paths. Of these paths, a total of 28 contained NMACs,

which originated from 10 encounter initializations. We analyzed the scenarios and confirmed that all were operationally rare scenarios. We present examples of NMAC found by the algorithm and discuss their properties.

Table 5: Differential stress testing configuration

Simulation	
number of simulators	2
number of aircraft per simulator	2
initialization	LLCEM
sensors	active, beacon-based, noiseless
collision avoidance system (test)	ACAS Xa Run 15 libcas 0.10.3
collision avoidance system (baseline)	TCAS II v7.1
pilot response model	deterministic 5s–3s
MCTS	
maximum steps	50
iterations	3000
exploration constant	100.0
$k$	0.5
$\alpha$	0.85

**ACAS X Issues RA, but TCAS Does Not.** We found some NMAC cases where ACAS X issued an RA but TCAS did not. An example is shown in Figure 10 where an NMAC occurs at 40 seconds in the ACAS X simulation but no NMAC occurs in the TCAS simulation. The encounter occurs with a probability density of  $1.7 \cdot 10^{-19}$ . No RA was issued in the TCAS simulation. In the example, both aircraft are traveling at a high absolute vertical rate exceeding 70 feet per second toward each other. Both aircraft receive an RA to level-off but the aircraft cannot respond in time due to the high vertical rates and the pilot response delay. The aircraft proceed to cross in altitude. After crossing, ACAS X increases the strength of the advisory in the same direction as the previous RA. Since the aircraft have crossed in altitude, responding to the RA results in a loss of vertical separation and an NMAC.

High vertical rates are known to make conflict resolution more difficult, especially for vertical-only collision avoidance systems like TCAS and this version of ACAS X. Later versions of ACAS X will issue advisories also in the horizontal direction. Aircraft with high vertical rates take longer to reverse direction vertically and more vertical distance is traveled during the pilot’s response delay. As a result, advisories take longer to take full effect. Moreover, in cases where both aircraft are maneuvering in the same vertical direction, an aircraft may lose the ability to “outrun” the other aircraft. For example, even if a maximal climb advisory is issued, it may not be sufficient for the aircraft to stay above a second aircraft climbing at an even higher rate. Another interesting feature of this encounter is the horizontal behavior. Aircraft 2 is initially turning away from the other aircraft before turning towards it at 8 seconds into the encounter. The initial RA is issued shortly after that maneuver. Large rapid changes in turn rate around the time of an RA can make it difficult for a collision avoidance system to accurately estimate the time to horizontal intersection.

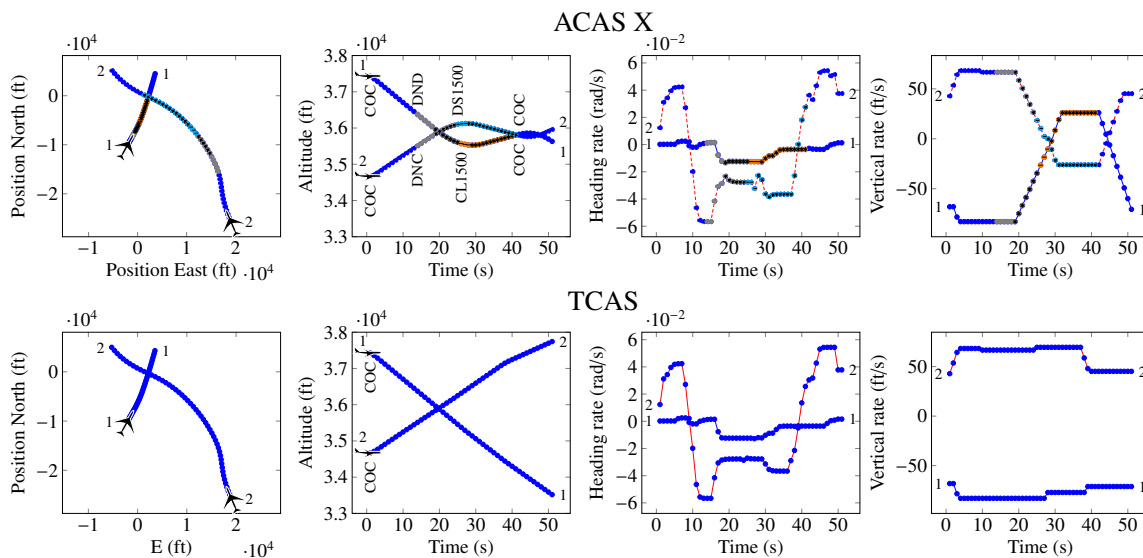


Figure 10: An encounter where ACAS X issues an RA but TCAS does not. The aircraft are initially traveling at high vertical rate and aircraft 2 also performs some horizontal maneuvering. An NMAC occurs in the ACAS X simulation at 40 seconds.

Overall, ACAS X is much safer and more operationally suitable than TCAS. However, there are some trade-offs between the two systems as highlighted by our methods. ACAS X's late altering characteristic, which reduces the number of unnecessary alerts, can sometimes hurt encounters with higher vertical rates, such as seen in this example. In deciding the trade-off, a designer must weigh the relative likelihood of these encounters versus the effect on other more frequently observed trajectories.

**Simultaneous Horizontal and Vertical Maneuvering.** Many of the NMAC encounters found involve an aircraft turning while simultaneously climbing or descending very rapidly. Figure 11 shows an example where an NMAC occurs at 45 seconds in the ACAS X simulation but no NMAC occurs in the TCAS simulation. The encounter occurs with probability density  $2.7 \cdot 10^{-4}$ . In this example, aircraft 1 is flying generally straight and level while aircraft 2 is simultaneously turning and climbing at a vertical rate exceeding 80 feet per second. Aircraft 2 receives an RA to level-off but is unable to maneuver in time before losing vertical separation resulting in an NMAC. In this example, TCAS is able to resolve the conflict by issuing RAs to both aircraft earlier in the encounter than ACAS X.

Horizontally, aircraft 2's turn quickly shortens the time to closest approach between the two aircraft. Vertically, aircraft 2 receives a level-off advisory but the high climb rate and pilot response delay limit how quickly the aircraft can be brought to compliance. Scenarios that involve turning and simultaneously climbing or descending at high rate are operationally very rare.

**Horizontal Maneuvering.** In some very rare cases, NMACs can also result from horizontal maneuvering alone. An example is shown in Figure 12 where an NMAC occurs at 40 seconds in the ACAS X simulation but no NMAC occurs in the TCAS simulation. The encounter occurs with probability density  $4.3 \cdot 10^{-11}$ . The aircraft are initially headed away from each other but they are also turning towards each other. At 25 seconds into the encounter, the aircraft turn more tightly



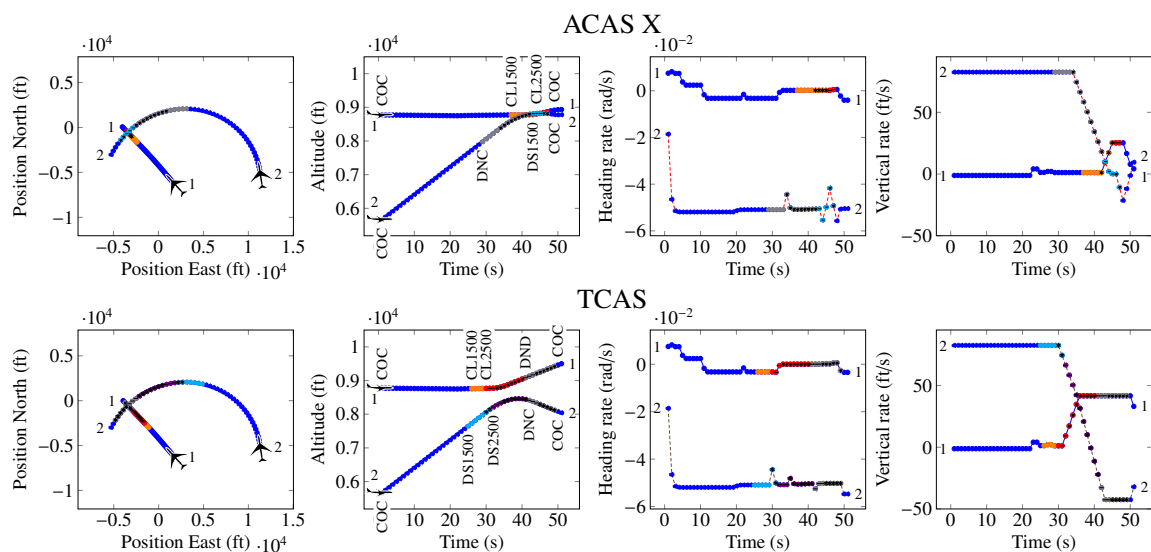


Figure 11: An NMAC encounter where one aircraft turns while simultaneously climbing very rapidly. An NMAC occurs in the ACAS X simulation at 45 seconds whereas no NMAC occurs in the TCAS simulation. Cases where aircraft maneuver both horizontally and vertically very rapidly are operationally very unlikely.

towards each other, rapidly reducing the time to closest approach. Crossing advisories are issued to the aircraft 9 seconds prior to NMAC. However, there is not enough time remaining to cross safely and an NMAC occurs. In this example, TCAS is able to resolve the conflict by issuing RAs to both aircraft earlier in the encounter. However, it is unclear how the aircraft got to their initial positions in the encounter and whether this initial position is generally reachable.

## 5.6 Performance Comparison with Direct Monte Carlo Simulation

We compare the performance of MCTS against direct Monte Carlo sampling given a fixed computational budget. The algorithms are given a fixed amount of wall clock time and the best path found at the end of that time is returned. We compare the wall clock time of the algorithms rather than number of samples to account for the additional computations performed in the MCTS algorithm. We use the same configuration as the single-threat encounter experiments as shown in Table 3 except that we limit the search based on computation time instead of a fixed number of iterations. The experiments were performed on a laptop with an Intel i7 4700HQ quad-core processor and 32 GB of memory.

Figure 13 shows the performance of the two algorithms as computation time varies. Figure 13a compares the total reward of the best encounters found by the algorithms. Each data point shows the mean and standard error of the mean of 100 pairwise encounters. Figure 13b shows the NMAC find rate of NMACs out of the 100 encounters searched. In both cases, MCTS clearly outperforms the baseline Monte Carlo search. The effectiveness of MCTS in finding NMACs is particularly important and we see that MCTS greatly outperforms the baseline in this regard. As the computational budget increases, MCTS is able to find increasingly many NMACs, whereas at the computational budgets considered, Monte Carlo is unable to find any NMACs.

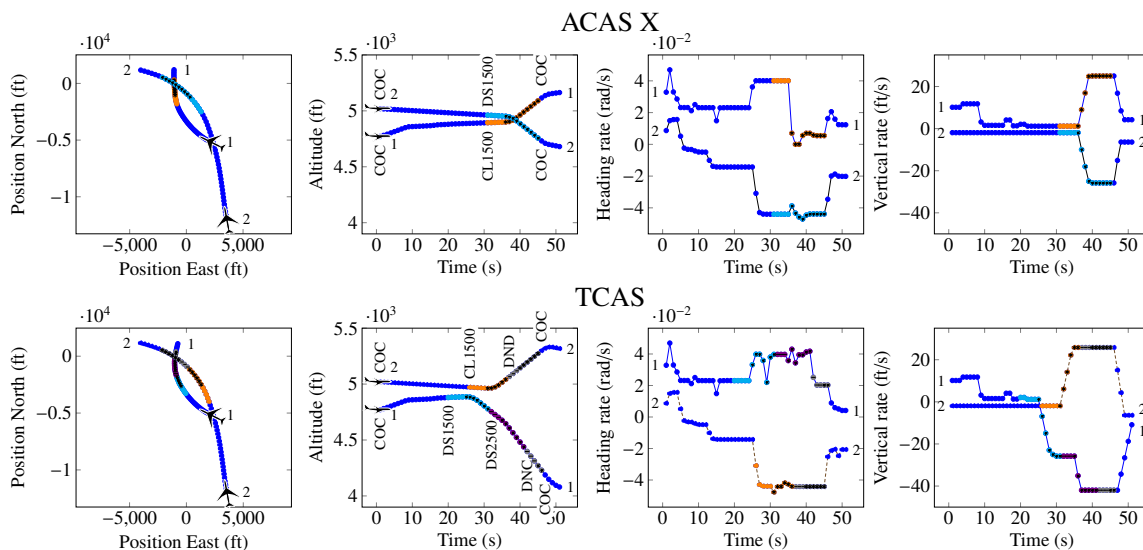


Figure 12: An NMAC encounter where the aircraft maneuver horizontally only. The aircraft start in an unlikely initial configuration. An NMAC occurs at 40 seconds in the ACAS X simulation but not in the TCAS simulation.

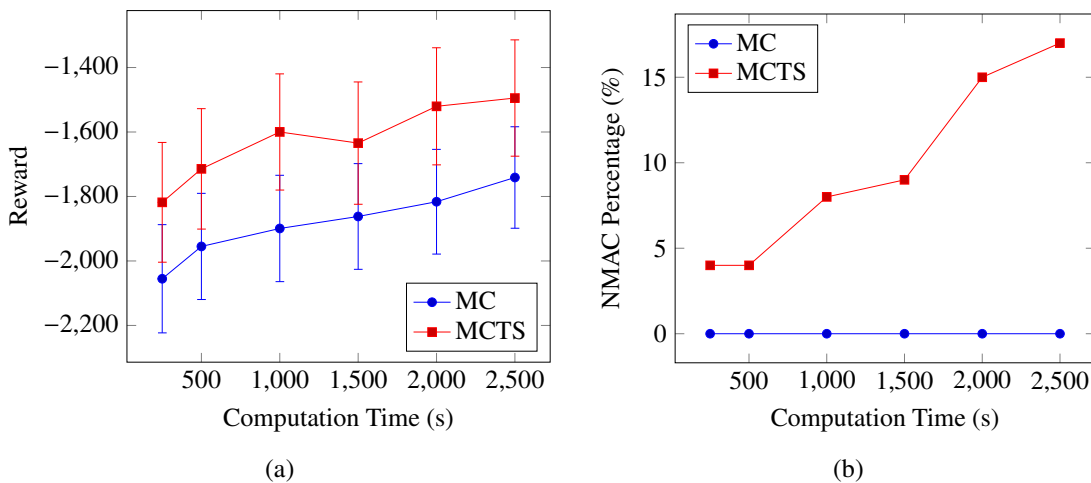


Figure 13: Performance of MCTS and Monte Carlo with computation time. MCTS is able to find an increasing number of NMACs while Monte Carlo is unable to find any due to the vast search space and rare failure events.

## 6. Conclusions

This paper presented adaptive stress testing (AST), a reinforcement learning-based stress testing approach for finding the most likely path to a failure event. We described AST formulations for the case where the state of the simulator is fully observable and also for the case where the part of all of the state may be hidden. For the latter case, we presented the MCTS-SA algorithm that uses the pseudorandom seed of the simulator to overcome partial observability. We also presented differ-

ential adaptive stress testing (DAST), an extension of AST for stress testing relative to a baseline. We applied AST and DAST to stress test a prototype of the next-generation ACAS X in an aircraft encounter simulator and successfully found a number of interesting examples of near mid-air collisions, which we reported to the ACAS X team for evaluation and to inform further development. Our implementation of AST is available as an open source Julia package at <https://github.com/sisl/AdaptiveStressTesting.jl>.

## Acknowledgments

We thank Neal Suchy at the Federal Aviation Administration; Robert Klaus and Cindy McLain at MIT Lincoln Laboratory; Rachel Szczesiul and Jeff Brush at Johns Hopkins Applied Physics Laboratory; and others in the ACAS X team. We thank Guillaume Brat at NASA Ames Research Center and Corina Pasareanu at Carnegie Mellon University Silicon Valley for their valuable feedback. This work was supported by the Safe and Autonomous Systems Operations (SASO) Project under NASA Aeronautics Research Mission Directorate (ARMD) Airspace Operations and Safety Program (AOSP); and also supported by the Federal Aviation Administration (FAA) Traffic-Alert & Collision Avoidance System (TCAS) Program Office (PO) AJM-233, Volpe National Transportation Systems Center Contract No. DTRT5715D30011.

## References

- Bouton, M., Nakhaei, A., Fujimura, K., & Kochenderfer, M. J. (2018). Scalable decision making with sensor occlusions for autonomous driving. In *IEEE International Conference on Robotics and Automation (ICRA)*.
- Browne, C. B., Powley, E., Whitehouse, D., Lucas, S. M., Cowling, P. I., Rohlfshagen, P., Tavener, S., Perez, D., Samothrakis, S., & Colton, S. (2012). A survey of Monte Carlo tree search methods. *IEEE Transactions on Computational Intelligence and AI in Games*, 4(1), 1–43.
- Chludzinski, B. J. (2009). Evaluation of TCAS II version 7.1 using the FAA fast-time encounter generator model. Project report ATC-346, Massachusetts Institute of Technology, Lincoln Laboratory.
- Couëtoux, A., Hoock, J.-B., Sokolovska, N., Teytaud, O., & Bonnard, N. (2011). Continuous upper confidence trees. In *Learning and Intelligent Optimization (LION)*, pp. 433–445.
- D’Silva, V., Kroening, D., & Weissenbacher, G. (2008). A survey of automated techniques for formal software verification. *IEEE Transactions on Computer-Aided Design of Integrated Circuits and Systems*, 27(7), 1165–1178.
- Federal Aviation Administration (2018). Next-generation airborne collision avoidance system (ACAS X) requirements matrix. RTCA (Unpublished).
- Gallier, J. H. (2015). *Logic for Computer Science: Foundations of Automatic Theorem Proving*. Courier Dover Publications.
- Gardner, R. W., Genin, D., McDowell, R., Rouff, C., Saksena, A., & Schmidt, A. (2016). Probabilistic model checking of the next-generation airborne collision avoidance system. In *Digital Avionics Systems Conference (DASC)*.

- Holland, J. E., Kochenderfer, M. J., & Olson, W. A. (2013). Optimizing the next generation collision avoidance system for safe, suitable, and acceptable operational performance. *Air Traffic Control Quarterly*, 21(3), 275–297.
- International Civil Aviation Organization (2007). Surveillance, radar and collision avoidance. In *International Standards and Recommended Practices* (4th edition), Vol. IV, annex 10.
- Jeannin, J.-B., Ghorbal, K., Kouskoulas, Y., Gardner, R., Schmidt, A., Zawadzki, E., & Platzer, A. (2015). A formally verified hybrid system for the next-generation airborne collision avoidance system. In *International Conference on Tools and Algorithms for the Construction and Analysis of Systems (TACAS)*.
- Katoen, J.-P. (2016). The probabilistic model checking landscape. In *ACM/IEEE Symposium on Logic in Computer Science*, pp. 31–45. ACM.
- Kern, C., & Greenstreet, M. R. (1999). Formal verification in hardware design: A survey. *ACM Transactions on Design Automation of Electronic Systems (TODAES)*, 4(2), 123–193.
- Kim, Y., & Kochenderfer, M. J. (2016). Improving aircraft collision risk estimation using the cross-entropy method. *Journal of Air Transportation*, 24(2), 55–62.
- Kochenderfer, M. J. (2015). *Decision Making under Uncertainty: Theory and Application*. MIT Press.
- Kochenderfer, M. J., & Chryssanthacopoulos, J. P. (2010). A decision-theoretic approach to developing robust collision avoidance logic. In *IEEE International Conference on Intelligent Transportation Systems (ITSC)*, pp. 1837–1842.
- Kochenderfer, M. J., Edwards, M. W. M., Espindle, L. P., Kuchar, J. K., & Griffith, J. D. (2010). Airspace encounter models for estimating collision risk. *AIAA Journal on Guidance, Control, and Dynamics*, 33(2), 487–499.
- Kochenderfer, M. J., Espindle, L. P., Kuchar, J. K., & Griffith, J. D. (2008). Correlated encounter model for cooperative aircraft in the national airspace system. Project report ATC-344, Massachusetts Institute of Technology, Lincoln Laboratory.
- Kochenderfer, M. J., Holland, J. E., & Chryssanthacopoulos, J. P. (2012). Next-generation airborne collision avoidance system. *Lincoln Laboratory Journal*, 19(1), 17–33.
- Kocsis, L., & Szepesvári, C. (2006). Bandit based Monte-Carlo planning. In *European Conference on Machine Learning (ECML)*, pp. 282–293.
- Koren, M., Alsaif, S., Lee, R., & Kochenderfer, M. J. (2018). Adaptive stress testing for autonomous vehicles. In *IEEE Intelligent Vehicles Symposium (IV)*.
- Kouskoulas, Y., Genin, D., Schmidt, A., & Jeannin, J. (2017). Formally verified safe vertical maneuvers for non-deterministic, accelerating aircraft dynamics. In *International Conference on Interactive Theorem Proving*, pp. 336–353.
- Kuchar, J. K., & Drumm, A. C. (2007). The traffic alert and collision avoidance system. *Lincoln Laboratory Journal*, 16(2), 277–296.
- Lee, R., Kochenderfer, M. J., Mengshoel, O. J., Brat, G. P., & Owen, M. P. (2015). Adaptive stress testing of airborne collision avoidance systems. In *AIAA/IEEE Digital Avionics Systems Conference (DASC)*.

- Lee, R., Kochenderfer, M. J., Mengshoel, O. J., & Silbermann, J. (2018). Interpretable categorization of heterogeneous time series data. In *SIAM International Conference on Data Mining (SDM)*. SIAM.
- Pargas, R. P., Harrold, M. J., & Peck, R. R. (1999). Test-data generation using genetic algorithms. *Software Testing, Verification and Reliability*, 9(4), 263–282.
- Pnueli, A. (1977). The temporal logic of programs. In *Foundations of Computer Science, 1977., 18th Annual Symposium on*, pp. 46–57. IEEE.
- Srivastava, P. R., & Kim, T.-h. (2009). Application of genetic algorithm in software testing. *International Journal of software Engineering and its Applications*, 3(4), 87–96.
- Sutton, R. S., & Barto, A. G. (1998). *Reinforcement Learning: An Introduction*. MIT Press, Cambridge, MA.
- von Essen, C., & Giannakopoulou, D. (2016). Probabilistic verification and synthesis of the next generation airborne collision avoidance system. *International Journal on Software Tools for Technology Transfer*, 18(2), 227–243.
- Watkins, C. J. C. H., & Dayan, P. (1992). Technical note: Q-learning. *Machine Learning*, 8, 279–292.
- Wiering, M., & van Otterlo, M. (Eds.). (2012). *Reinforcement Learning: State of the Art*. Springer, New York.